Table II. Jump Angles vs. Position in Phase II of Heneicosane

position	33 °C	39 °C	41 °C
2	83.0	85.0	89.5
4	81.8	84.7	
6	82.0	84.7	87.4
11	82.2	83.5	86.4

is reduced the torsion is frozen out, and it is absent at position 4 at 0 °C and position 2 at −20 °C.

In phase II infrared spectroscopy has demonstrated the existence of a positional- and temperature-dependent population of gauche rotamers. Table I lists these populations, together with those which would be estimated on the basis of the reduction in the V_{YY}^{J} spectral features shown in Figure 5.[19] There is quite good agreement, and it is apparent that substantial off-axis motion occurs in phase II and that it can be largely attributed to the introduction of gauche rotamers.

However, even with gauche rotamers taken into account, the spectra are still typical of $C-^2H_2$ groups undergoing hindered rotation.[8] This is particularly well demonstrated for the C_{21}-*11,11-d*$_2$ spectra, where η is large, and decreases with increasing temperature, while the average gauche population is very low and varies from 0.4% to 0.8%. The phase II spectra were thus simulated by using the restricted jump model, having first assumed that trans-gauche isomerization had modulated the electric field gradient tensor. The results of the simulations of C_{21}-*2,2-d*$_2$ spectra are shown in Figure 6, while Table II lists the jump angles required as a function of temperature and position. Near $T_{I\rightarrow II}$ the jump angle is virtually constant in positions 4–18, but larger at positions 2 and 20. As the temperature is increased to 41 °C the jump angle at position 2 and 20 increases by 6.5° compared to 4.2° at position 11. These data indicate that the predominant motions in phase II are hindered rotation and fast trans-gauche isomerization.

We should emphasize that the two site jump model employed here is only one of several possible choices.[17,23] For example, jumps of fixed angle between states of variable population could yield similar spectra. As yet there appears to be no means to distinguish unequivocally between these models. The derived θ values must therefore be considered as empirical parameters useful for comparison of behavior at different positions and temperatures. However, our analysis in terms of two types of motion, rapid gauche-trans interconversion, and limited torsional oscillation is unequivocal.

Recent X-ray studies of *n*-alkanes[4] have demonstrated that, within phase II, the cross-sectional area of the unit cell increases as the temperature is raised, permitting more mobility about the long axis. The rate of change of the ratio a/b, where a and b are the unit cell dimensions, is nonlinear and correlates with the nonlinear rate of change of η (Figure 4). We have also found that in phase II the rate of introduction of gauche rotamers into the 2 position of 2,2-dideuterionononadecane is nonliner, increasing with increasing temperature.[20] This suggests that all three effects are interrelated, but the causative factor remains unexplained, particularly as recent studies have demonstrated further weak transitions within phase II.[21,22]

Conclusion

When considered in conjunction with the evidence for a negligible phase I gauche population, the ^2H NMR spectra of the selectivity deuterated heneicosanes indicate that in this phase the C_6–C_{16} segment of the chain is rigidly packed and immobile on a time scale of 10^5 s^{-1}. However, there is present a torsional motion in the C_5–C_1 and C_{17}–C_{21} segments, with an amplitude of 10–20° at temperatures just below $T_{I\rightarrow II}$. As the temperature is reduced the amplitude of the torsion decreases, and it is not present below −30 °C.

Recent studies have shown that the phase II structure and dynamics are complex, and temperature dependent. These data indicate that temperature-dependent, hindered rotation and fast trans-gauche isomerization are the principle disordering mechanisms in phase II.

Registry No. $CH_3CD_2(CH_2)_{18}CH_3$, 86369-65-5; $CH_3(CH_2)_2CD_2(CH_2)_{16}CH_3$, 84010-39-9; $CH_3(CH_2)_4CD_2(CH_2)_{14}CH_3$, 86369-66-6; $CH_3(CH_2)_9CD_2(CH_2)_9CH_3$, 86369-67-7.

(19) The gauche populations were estimated by comparing our measured V_{YY}^{J} components with the quadrupole splittings determined in simulations of specifically deuterated phosphatidylethanolamine (PE) acyl chains in their gel state (see ref 17). These simulations had PE undergoing 120° rotational jumps about the long axis, with fast trans-gauche isomerization superimposed. Rapid 120° jumps will not affect V_{YY} (or V_{YY}^{J}) and will leave it as the largest spectral feature in the spectrum of gel-state PE. However, rapid jumps between a trans orientation ($C-^2H$ at 90° to the long axis) and a gauche orientation ($C-^2H$ at 35.3° to the long axis) will modulate V_{YY}^{J}. Gauche populations of approximately 7% were sufficient to reduce V_{YY}^{J} by 21 kHz from the rigid limit spectrum of PE.

(20) Cameron, D. G.; Casal, H. L.; Synder, R. G.; Maroncelli, H., unpublished observations.

(21) Doucet, J.; Denicolo, I.; Craievich, A.; Collet, A. *J. Chem. Phys.* **1981**, *75*, 5125.

(22) Ungar, G. *J. Phys. Chem.* **1983**, *87*, 689.

(23) Spiess, H. W. In "NMR Basic Principles and Progress"; Diehl, P., Fluck, E., and Kosfield, R., Eds.; Springer: Berlin, 1978; Vol. 15, pp 55–214.

The Distribution of Carbon in Boron Carbide: A ^{13}C Nuclear Magnetic Resonance Study

T. M. Duncan

Contribution from AT&T Bell Laboratories, Murray Hill, New Jersey 07974.
Received September 19, 1983

Abstract: The symmetry and local bonding of carbon in boron carbide ($B_{12}C_3$) are studied with ^{13}C nuclear magnetic resonance (NMR) spectroscopy. The $^{13}C-^{11}B$ heteronuclear dipolar couplings determined from the results of spin–echo experiments indicate that carbon is present only as C_3 chains. That is, there is no evidence of boron substituting for the middle carbon atom in the chain. The chemical shift powder patterns resolved from the experimental spectra indicate environments consistent with the assignments based on dipolar couplings. From the spectral assignments made in this study it is proposed that the distribution of carbon in samples of boron carbide can be determined from the isotropic shifts resolved by magic-angle spinning. In addition, this study demonstrates the applicability of a spin-diffusion model to analyze heteronuclear couplings and presents a formalism to separate overlapping spectra.

The crystal structure of boron carbide, $B_{12}C_3$, as proposed originally from X-ray diffraction studies,[1,2] is a rhombohedral arrangement of two structural units: icosahedra of boron atoms and linear chains of three carbon atoms. The boron atoms are

0002-7863/84/1506-2270$01.50/0

each sixfold coordinated, with five of the bonds to other boron atoms in the same icosahedron. Half of the boron atoms (in $6h_2$ sites) form a sixth bond to boron atoms of neighboring icosahedra whereas the other boron atoms (in $6h_1$ sites) bond to carbon in 2c positions. Both boron sites are approximately centered in pentagonal pyramids. The carbon atoms at the ends of the linear chains (2c sites) are fourfold coordinated to three boron atoms and to the carbon in the 1b position at the middle of the chain. The 1b carbon atom is bonded only to the two carbon atoms at the ends of the chain. The C_3 chains are isolated from each other whereas the boron atoms form a continuous network throughout the lattice.

The rhombohedral structure of boron carbide is unaltered by variations in stoichiometry in the range 6–24 atom%.[3] It is proposed that in boron-rich compositions, the 1b lattice site at the middle of the linear chain may be occupied by boron,[2-7] yielding a structure referred to as $B_{12}(CBC)$, which is reported to be the more thermally stable form of boron carbide[8] and is the third hardest of all known compounds.[9] $B_{13}C_2$ has enhanced stability because boron atoms are better suited for the 1b position, which forms only two covalent bonds. Carbon-rich compositions may lead either to be formation of graphite impurities[10] or, it is proposed,[11] may result in structures in which carbon atoms substitute for boron atoms in the $6h_2$ sites of the icosahedra. Finally, it is suggested that both types of substitution occur in stoichiometric compounds of $B_{12}C_3$.[11] Specifically, it is suggested that $B_{12}C_3$ exists as a solid solution that ranges in local composition between $B_{12}(CBC)$ and $B_6C_6(CBC)$.[11]

X-ray diffraction studies yield unambiguous determinations of the overall crystal structure of boron carbide, but since the ^{11}B and ^{12}C have similar electron densities, it is difficult to determine whether the lattice sites contain boron or carbon atoms. The differences in electron densities are also reduced by charge transfer, which results in a structure represented as $(B_{12})^{2-}(C_3)^{2+}$. Conversely, nuclear magnetic resonance (NMR) spectroscopy measures interactions that are insensitive to long-range order but can easily differentiate between sites of different symmetry and bonding-coordination number.

This study details the analysis of the ^{13}C NMR spectra of boron carbide. The dominant broadening in the ^{13}C NMR spectra of boron carbide is due to the dipolar coupling to ^{11}B and, to a lesser degree, to ^{10}B. Thus, in principle, the ^{13}C spectrum of each carbon site may be identified by the number of and distance to nearest boron neighbors, as calculated from the Van Vleck equation.[12] One would also predict a different isotropic chemical shift for the ^{13}C NMR spectrum of each carbon site, which could be correlated to the number and type of nearest boron atoms. Similar distributions in the isotropic chemical shifts of ^{29}Si NMR spectra of zeolites resolved by "magic-angle" spinning have proven useful in determining the number of nearest aluminum neighbors.[13] In addition, the orientational anisotropy of the chemical shift spectrum measured with stationary samples reflect the symmetry of the carbon position in the lattice. Finally, the absolute spectral intensities yield quantitative information on the amount of each carbon species.

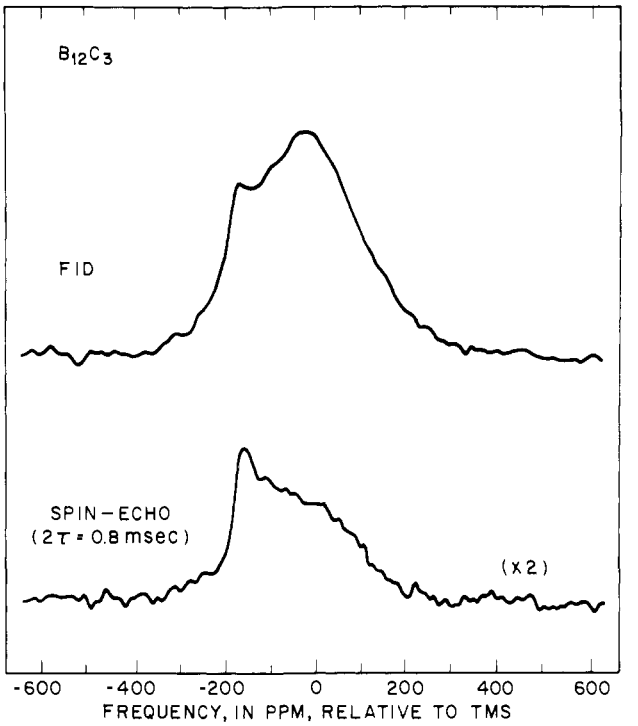

Figure 1. ^{13}C NMR spectra of $B_{12}C_3$ at 295 K, obtained by Fourier transforming a free induction decay (FID) and an echo after a delay of 0.8 ms.

A previous study of the ^{11}B NMR spectra of boron carbide demonstrated the ability of the technique to distinguish different sites in the lattice.[14] Three distinct types of boron positions, identified by differences in quadrupolar couplings, were assigned to the $6h_1$ and $6h_2$ sites and to boron substituted into the 1b carbon positions. The ^{11}B NMR spectrum of the 1b boron was characterized by a relatively strong quadrupolar coupling (5.6 MHz) and threefold rotational symmetry. The relative intensities of the peaks in the spectra of single crystals of boron carbide, presumed to be boron rich, indicated that at least 60% of the 1b positions contained boron.

Experimental Section

The ^{13}C NMR spectra were measured at 50.35 MHz on a Bruker CXP-200 spectrometer. To reduce the recovery time following a 90° pulse, the quadrature-detected free-induction decays (FID's) were obtained by alternately adding and subtracting the transients observed after a 90° pulse and after a [(180° pulse–(delay 5 ms)–(90° pulse)] sequence. The spin–lattice relaxation time (T_1) was determined by the saturation–recovery technique.[15] The spin–echo spectra were obtained by Fourier-transforming the echo detected after a [(90° pulse)–τ–(180° pulse)–τ–observe] sequence.[15] The ^{13}C NMR spectra were also measured with samples spinning at the "magic angle" relative to the external magnetic field to remove the broadening caused by chemical shift anisotropy and dipolar interactions.[16] The angle of the rotation axis was determined by optimizing the ^{79}Br spectrum of KBr.[17] The strengths of the excitation pulses were about 100 G, which is sufficient to excite uniformily the spectral range –600 to 600 ppm. The ^{13}C NMR spectra are reported on the σ scale for chemical shifts, relative to tetramethylsilane (Me_4Si) (i.e., benzene lies at –128.7 ppm and "downfield" is to the left).

Samples of boron carbide were obtained from Alfa and from Pfaltz and Bauer in powders as particles smaller than 325 mesh (45 μm). The

(1) Zhdanov, G. S.; Sevast'yanov, N. G. *C. R. Acad. Sci. URSS* **1941**, *32*, 432.
(2) Clark, H. K.; Hoard, J. L. *J. Am. Chem. Soc.* **1943**, *65*, 2115.
(3) Hoard, J. L.; Hughes, R. E. In "The Chemistry of Boron and Its Compounds"; Muetterties, E. L., Ed.; Wiley: New York, 1967; pp 25–154.
(4) Zhdanov, G. S.; Zhuraleve, N. N.; Zevin, D. S. *Dokl. Akad. Nauk. SSSR* **1953**, *92*, 767.
(5) Allen, R. D. *J. Am. Chem. Soc.* **1953**, *75*, 3582.
(6) Lipp, A. *Ber. Dtsch. Keram. Ges.* **1966**, *43*, 60.
(7) Yakel, H. L. *Acta Crystallogr., Sect. B* **1975**, *31*, 1797.
(8) Zhdanov, G. S.; Meerson, G. A.; Zhuralev, N. N.; Samsonov, G. V. *Zh. Fiz. Kim.* **1954**, *28*, 1076.
(9) Naslain, R. In "Boron and Refractory Borides"; Matkovich, V. I., Ed.; Springer-Verlag: New York, 1977; Chapter X.
(10) (a) Ruste, J.; Bouchacourt, M.; Thevenot, F. *J. Less-Common Met.* **1978**, *59*, 131. (b) Beauvy, M.; Angers, R. *Ibid.* **1981**, *80*, 227.
(11) Matkovich, V. I.; Economy, J. In "Boron and Refractory Borides"; Matkovich, V. I., Ed.; Springer-Verlag: New York, 1977; Chapter VII.
(12) Abragram, A. "The Principles of Nuclear Magnetism"; Oxford Press: London, 1961.
(13) See, for example: (a) Lippmaa, E.; Magi, M.; Samoson, A.; Tarmak, M.; Englehardt, G. *J. Am. Chem. Soc.* **1981**, *103*, 4992. (b) Klinowski, J.; Thomas, J. M.; Fyfe, C. A.; Hartman, J. S. *J. Phys. Chem.* **1981**, *85*, 2590.
(14) Silver, A. H.; Bray, P. J. *J. Chem. Phys.* **1959**, *31*, 247.
(15) Slichter, C. P. "Principles of Magnetic Resonance", 2nd ed.; Springer-Verlag: New York, 1978.
(16) Andrew, E. R. *Prog. Nucl. Reson. Spectrosc.* **1971**, *8*, 1. (b) Stejskal, E. O.; Schaefer, J.; McKay, R. A. *J. Magn. Reson.* **1977**, *25*, 569.
(17) Frye, J. S.; Maciel, G. E. *J. Magn. Reson.* **1982**, *48*, 125.

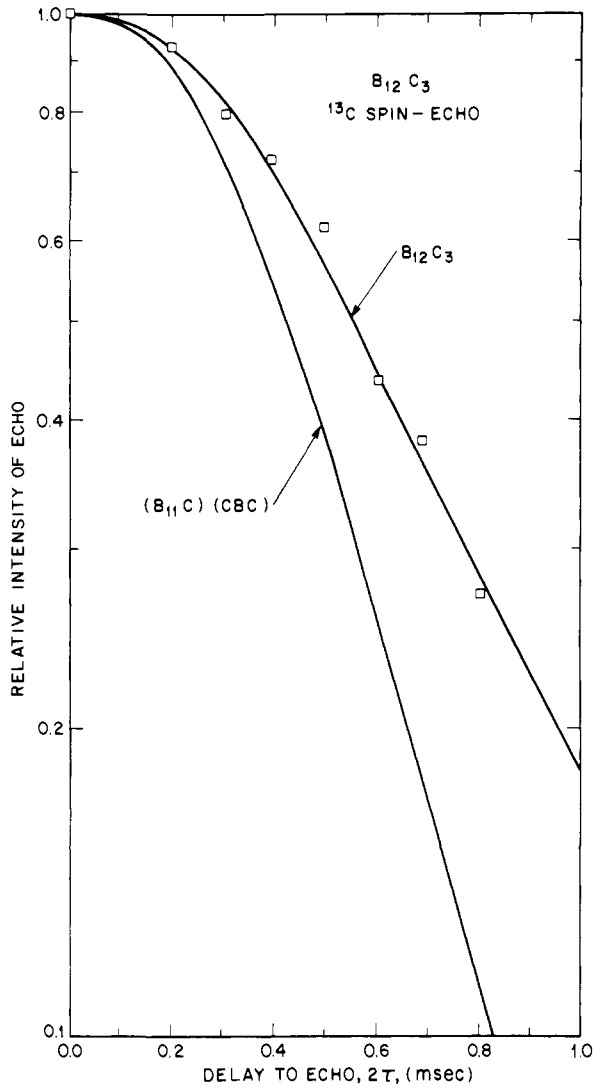

Figure 2. Integrated intensity of the ^{13}C NMR spectrum of $B_{12}C_3$ as a function of the length of delay (2τ) in the spin-echo experiment. The calculated curves are treated under Discussion.

composition of the material from Alfa was quoted to be 77.54% boron, which is only slightly less than the $B_{12}C_3$ stoichiometric value of 78.25%. The ^{13}C NMR spectra were independent of the source of the sample.

Results

The ^{13}C NMR spectrum of polycrystalline $B_{12}C_3$, shown in Figure 1, is quite broad, relative to the spectra of organic compounds. The ^{13}C T_1 is 16 ± 2 s at 295 K, and the integrated intensity of the spectrum, calibrated with standard samples of adamantane and silicon carbide, indicates that the spectrum represents at least 97% of the carbon in the sample. Thus, regardless of the distribution of carbon in the lattice, the FID spectrum is the superposition of at least two line shapes that correspond to different sites in the lattice. Evidence of multiple, overlapping spectra is revealed with the spin-echo experiment. As the delay to the echo (2τ) is increased, the center-of-mass of the spectrum shifts downfield, from −31 ± 10 ppm for the FID to −65 ± 10 ppm for the echo at 0.8 ms, shown in Figure 1. In addition, the shape of the spectrum changes: the peak at −200 ppm persists whereas the broad absorption centered at ~0 ppm decreases. Figure 2 shows the intensity of the spectra as a function of the delay to the echo. Each of the spectra in Figure 1 and the spectra measured to determine the decay in Figure 2 are the accumulation of about 1500 scans required at a rate of 1 min^{-1}.

Figure 3 shows the spectrum of boron carbide acquired by rotating the sample about the "magic angle" at 3900 Hz in a delrin rotor. The FID was observed while the sample was irradiated at 200.14 MHz to suppress the coupling to ^1H nuclei. Although

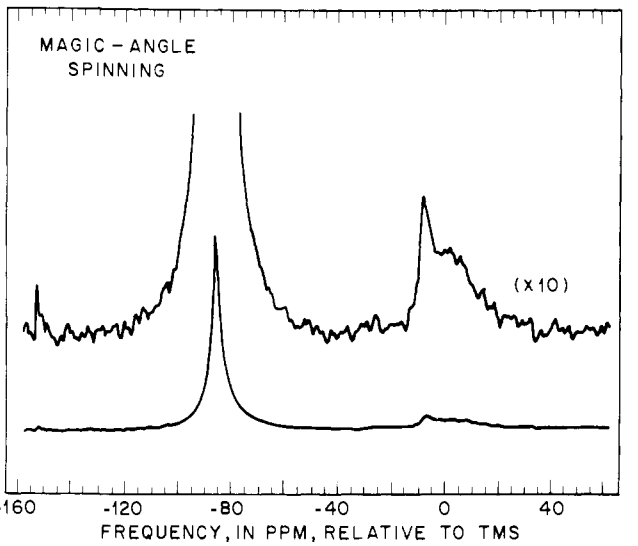

Figure 3. ^{13}C NMR spectrum of $B_{12}C_3$, spinning at the magic angle at 3900 Hz in a delrin rotor. The intense peak at −88 ppm and the sideband at −10 ppm are caused by delrin.

the decoupling is inconsequential to the ^{13}C NMR spectrum of boron carbide, it was necessary to sharpen the background delrin signal, which consists of an intense peak at −88 ppm with a sideband at −10 ppm. A third feature in Figure 3, not present at slower spinning rates or with an empty rotor, is a relatively broad peak that lies slightly upfield of the delrin sideband at ~−2 ppm.

Discussion

A. Analysis of Spin-Echo Data. The decrease in intensities of the ^{13}C NMR spectra as a function of the echo delay is caused by a loss of phase coherence in the ensemble of ^{13}C nuclear magnetic moments. Dephasing is caused by variations in the local magnetic fields. Spatial variations, such as chemical shift anisotropy and field inhomogeneity, are refocussed by the spin-echo sequence and thus do not contribute to the rate of decay. Random fluctuations of local fields, in particular, variations resulting from spin diffusion within a dipolar-coupled spin ensemble, are not refocused. The most pronounced effect occurs when the time constant for spin diffusion is comparable to the delay to the echo. Because of low isotopic abundance, the ^{13}C–^{13}C homonuclear dipolar coupling is only about 0.21 kHz and thus may be neglected in this study. The dominant factor in the decay of the ^{13}C spin-echo intensity is the heteronuclear dipolar coupling to ^{11}B.

An expression for the decay of the spin-echo intensity of a spin system with weak homonuclear coupling (e.g., ^{13}C), coupled to a second spin system with strong homonuclear coupling (e.g., ^{11}B), was recently derived for isolated ^{31}P nuclei in contact with clusters of ^1H nuclei.[18] It was shown that the intensity of the echo at time 2τ is given by eq 1, where $\langle\Phi^2\rangle$ is the mean-squared phase

$$M(2\tau) = M(0)e^{-\langle\Phi^2\rangle} \quad (1)$$

angle of the ^{13}C magnetization, given by eq 2, where $T_{2,S}$ is the

$$\langle\Phi^2\rangle = \frac{2T^2_{2,S}}{T^2_{2,IS}}\left[2\left(\frac{\tau}{T_{2,S}}\right) + 4e^{-\tau/T_{2,S}} - e^{-2\tau/T_{2,S}} - 3\right] \quad (2)$$

time constant for spin–spin relaxation in the second spin system, ^{11}B, and $T_{2,IS}$ is the time constant for the heteronuclear coupling between ^{13}C and ^{11}B. The model assumes an exponential correlation function for the z components of the ^{11}B magnetization and neglects the effects of concerted ^{11}B–^{11}B spin flips.

From the interatomic spacing in various crystal structures proposed for boron carbide, the approximate relaxation time constants in eq 2 may be calculated from the Van Vleck equation. The Van Vleck equation applies to nuclear spins in the high-field

(18) Reimer, J. A.; Duncan, T. M. *Phys. Rev. B* **1983**, *27*, 4895.

Table I. $^{13}C-^{11}B$ Heteronuclear Dipolar Interactions

structure	carbon position	distance to boron site,[a] Å	no. of boron sites	$^{13}C-^{11}B$ heteronuclear coupling,[b] kHz
$B_{12}C_3$	2c	1.60	3	3.90
		2.95	15	
	1b	2.33	6	2.19
		2.78	12	
$(B_{11}C)(CBC)$	2c	1.44	1	4.90
		1.60	3	
		2.95	15	
	$6h_2$	1.72	1	3.79
		1.79	5	

[a] Interatomic distances from ref 3, 7, and 11. [b] Square root of the second moment of the dipolar interaction calculated from the Van Vleck equation; the $^{13}C-^{10}B$ interaction is a factor of 0.30 smaller.

limit, and therefore care must be taken in calculating second moments for quadrupolar nuclei, such as ^{11}B or ^{10}B. However, boron occupies a highly symmetric site in the lattice, and therefore small electrostatic field gradients would be predicted. Indeed, the ^{10}B NMR spectrum of $B_{12}C_3$ has a half-width at half-maximum of 45 kHz,[19] which is a relatively weak quadrupolar splitting. Furthermore, the integrated intensity of the ^{10}B spectrum assured that boron atoms in both $6h_1$ and $6h_2$ sites were contributing to the peak. Also, the quadrupolar splitting of the ^{11}B spectrum of boron carbide has been determined from the second-order shift in the central transition ($m = {}^1/_2 \leftrightarrow -{}^1/_2$).[14] The ^{11}B quadrupolar coupling (eqQ) for the $6h_1$ boron site was estimated to lie in the range 0.2–0.7 MHz and the $6h_2$ position was determined to have a splitting of 1.3 ± 0.1 MHz.[14] Therefore, it is assumed that the ^{11}B nuclei, which resonate at 64.2 MHz in the field used here, are in Zeeman states and the Van Vleck equation is applicable. The time constants for the homonuclear ^{11}B couplings, calculated as the inverse of the square roots of the second moments, are 1.40×10^{-4} and 1.56×10^{-4} s, for the $6h_2$ and $6h_1$ sites, respectively.

Similarly, time constants for the $^{13}C-^{11}B$ interactions may be calculated from the interatomic distances determined by X-ray diffraction studies.[3,7,11] Two crystal structures with the formula $B_{12}C_3$ will be considered here: the original structure composed of boron icosahedra and linear carbon chains, and a modification in which a boron atom from a $6h_1$ site is interchanged with the middle carbon atom $(B_{11}C)(CBC)$. The choice of models is appropriate because X-ray diffraction studies detect negligible anisotropy in the apparent thermal motions of the 2c carbon sites, which was interpreted as structural and chemical homogeneity of the linear chains.[3] Thus, it was suggested that the linear chains in boron carbide are either CBC or C_3, but not a mixture.[3] The $^{13}C-^{11}B$ heteronuclear dipolar couplings for each site in the two models are presented in Table I.

The intensity of the ^{13}C magnetization observed with the spin–echo sequence may be expressed as in eq 3, where $M_a(0)$

$$M(2\tau) = M_a(0)e^{-\langle\Phi_a^2\rangle} + M_b(0)e^{-\langle\Phi_b^2\rangle} \quad (3)$$

and $M_b(0)$ are initial populations of carbon in sites a and b. Site a is arbitrarily assigned to the carbon position with the stronger heteronuclear coupling. For example, for the $B_{12}C_3$ structure, site a is the 2c position and site b is the 1b position. In either model, $M_a(0) = {}^2/_3$ and $M_b(0) = {}^1/_3$. The mean-squared phase angles for the ^{13}C nuclei at sites a and b are given by $\langle\Phi_a^2\rangle$ and $\langle\Phi_b^2\rangle$, which can be calculated from eq 2 and the data in Table I.

Figure 2 shows the theoretical spin–echo decays predicted for the $B_{12}C_3$ and $(B_{11}C)(CBC)$ forms of boron carbide calculated from the dephasing effects of ^{11}B nuclei. The $^{10}B-^{13}C$ interaction, calculated from the same formalism, further decreases the echo intensity at 1.0 ms by less than 5%. Clearly, the experimental results indicate that the structure of boron carbide in these samples is $B_{12}C_3$, as proposed originally.[1,2] The spin–echo decay for $B_{12}C_3$ with a fraction of the 1b sites occupied by boron would be a linear combination of the two curves in Figure 2. These data suggest that not more than 10% of the 1b sites contain boron atoms.

B. Resolution of Overlapping ^{13}C Spectra. In general, the ^{13}C chemical shift powder pattern reflects the anisotropy and symmetry at a lattice site and therefore is helpful in analyzing spectral assignments. Unfortunately, the ^{13}C spectra for the two lattice sites in boron carbide overlap in the spectra in Figure 1. However, since the ^{13}C nuclei in different lattice sites have different $^{13}C-^{11}B$ couplings and different T_2's, it is possible to separate the individual spectra of the sites, as follows. The relative contributions to the experimental spectra from sites a and b change as the echo delay is increased, as expressed in eq 3. For example, the spectrum obtained from the FID is the superposition of the spectra of sites a and b, and thus the ratio of intensities is 2:1. At time $2\tau = 0.8$ ms, the exponential factors in eq 3 for sites a and b are 0.17 and 0.57, respectively. Therefore, in the spectrum obtained from the spin–echo at 0.8 ms shown in Figure 1, the ratio of site a and site b has been reduced to 0.60:1.

The spectra of sites a and b may be resolved by analyzing the experimental spectra in Figure 1 and the spectra corresponding to the data in Figure 2. The spectral intensity of the FID spectrum at frequency ν is the superposition of the intensity from the signals at the two carbon sites, a and b, as stated in eq 4, where $I(\nu,0)$

$$I(\nu,0) = I_a(\nu,0) + I_b(\nu,0) \quad (4)$$

is the observed intensity at $2\tau = 0$ ms (i.e., a FID is an echo with zero delay). The spectrum obtained from an echo at 2τ is also the sum of the spectra of sites a and b, which can be expressed in terms of the FID spectrum, as in eq 5. The exponential terms

$$\begin{aligned} I(\nu,2\tau) &= I_a(\nu,2\tau) + I_b(\nu,2\tau) \\ &= I_a(\nu,0)e^{-\langle\Phi_a^2\rangle} + I_b(\nu,0)e^{-\langle\Phi_b^2\rangle} \end{aligned} \quad (5)$$

are the same as those in the expression for the integrated intensity in eq 3. Thus, the spectra from the FID and echoes at seven different delays yield eight linear equations of the form in eq 5. Expressions for the spectra of sites a and b are determined by a least-squares regression and are given in eq 6 and 7, such that

$$\begin{aligned} I_a(\nu,0) = \\ \{[\textstyle\sum I(\nu,2\tau)e^{-\langle\Phi_a^2\rangle}][\sum e^{-2\langle\Phi_b^2\rangle}] - [\sum I(\nu,2\tau)e^{-\langle\Phi_b^2\rangle}] \times \\ [\textstyle\sum e^{-(\langle\Phi_a^2\rangle+\langle\Phi_b^2\rangle)}]\}/\{[\sum e^{-2\langle\Phi_a^2\rangle}][\sum e^{-2\langle\Phi_b^2\rangle}] - [\sum e^{-(\langle\Phi_a^2\rangle+\langle\Phi_b^2\rangle)}]^2\} \end{aligned} \quad (6)$$

$$I_b(\nu,0) = \frac{\sum I(\nu,2\tau)e^{-\langle\Phi_a^2\rangle} - I_a(\nu,0)\sum e^{-2\langle\Phi_a^2\rangle}}{\sum e^{-(\langle\Phi_a^2\rangle + \langle\Phi_b^2\rangle)}} \quad (7)$$

each summation is over the eight values of 2τ from 0 to 0.8 ms.

Figure 4 shows the spectra of sites a and b calculated from eq 6 and 7. Spectrum a corresponds to 2c carbon atoms at the ends of the linear chain and spectrum b is attributed to the 1b sites. The ratio of the areas of the spectra, which is not assumed in the above calculation, is 1.96:1.0.

C. Interpretation of ^{13}C Spectra. The resolved spectra of the two carbon species in boron carbide are fit with theoretical chemical shift power patterns,[20] given by the solid lines in Figure 4. The spectrum assigned to the 2c carbon (site a) has an isotropic shift of -13 ± 15 ppm. The least-squares fit to the spectrum yields principal components at -145, 44, and 60 ± 25 ppm and a Guassian broadening of half-width 5.20 kHz. The spectrum in Figure 4 assigned to the 1b carbon atoms (site b) has an isotropic shift of -85 ± 10 ppm and principal components of -190, -170, and 105 ± 15 ppm and is convoluted with a Gaussian broadening function of half-width 1.59 kHz. Table II contains a summary of the ^{13}C NMR parameters.

Spectrum b in Figure 4 displays clearly the positions of the shoulders and yields an unambiguous theoretical fit. In spectrum a, however, the shoulders are not obvious because the dipolar

(19) Duncan, T. M., unpublished results.

(20) Bloembergen, N.; Rowland, J. A. *Acta Metall.* **1953**, *1*, 731.

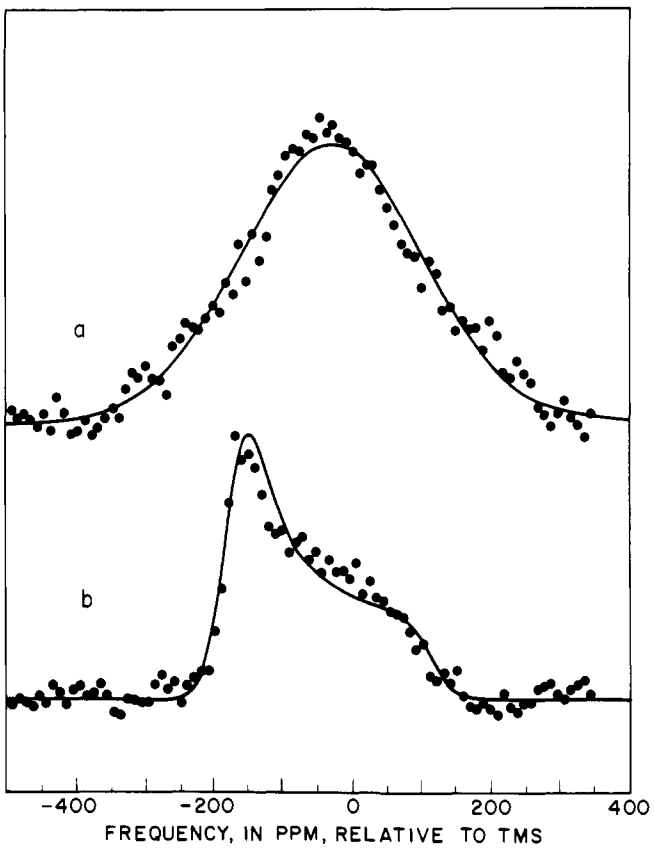

Figure 4. ^{13}C NMR spectra resolved by separating the spin–echo spectra into species with (a) relatively strong and (b) moderate heteronuclear coupling to ^{11}B. The solid curves are least-squares fits to theoretical chemical shift powder patterns.

Table II. Summary of ^{13}C NMR Parameters for $B_{12}C_3$

carbon site	chemical shift parameters[a] isotropic shift	principal components σ_{11}	σ_{22}	σ_{33}	dipolar broadening, kHz exptl[b]	calcd[c]
2c	−13 ± 15	−145	45	60	5.20	4.07
1b	−85 ± 10	−190	−170	105	1.59	2.29

[a] In ppm, relative to Me_4Si. [b] Half-width of Gaussian broadening convoluted into the powder pattern as determined by least-squares fit. [c] Square root of the second moment of the $^{13}C-^{11}B$ and $^{13}C-^{10}B$ dipolar interactions calculated from the Van Vleck equation.

broadening is greater than the chemical shift anisotropy, and therefore it is not possible to obtain a unique theoretical fit to a powder pattern. Thus, the values in Table II for the 2c carbon should be regarded as approximate. However, although the determination of exact chemical shielding components for spectrum a is tenuous, it is reasonably certain that the components perpendicular to the symmetry axis lie upfield.

The two downfield components of the spectrum assigned to the 1b carbon position (Figure 4b) are nearly equal, which implies an environment with at least threefold symmetry about an axis.[21] The shielding perpendicular to the axis of symmetry is downfield, which is also the case for carbon compounds in axially symmetric environments, with bonds only along the axis of symmetry. Examples of these compounds are acetylene[22] and inorganic acetylides (CaC_2, SrC_2, and BaC_2).[23] Conversely, carbon atoms with axially symmetric shielding, but with bonds perpendicular to the symmetry axis, such as graphite or tungsten carbide, have chemical shift powder patterns with opposite orientation; the chemical shielding perpendicular to the symmetry axis is upfield from the isotropic shift. In addition, the width of the chemical shift spectrum of the 1b carbon of boron carbide (285 ppm) is comparable to the shielding anisotropy of other unsaturated carbons, such as acetylene (240 ppm),[22] CaC_2 (350 ppm), SrC_2 (320 ppm), and BaC_2 (270 ppm).

Figure 4a represents carbon species in boron carbide with strong $^{13}C-^{11}B$ dipolar interactions and is consistent with the bonding at the 2c sites. First, the chemical anisotropy is less than that of 1b positions, as expected. The 2c site can be approximated as the center of a trigonal pyramid, whereas the 1b site forms bonds only along the symmetry axis. Second, the orientation of the chemical shielding of the 2c spectrum is the opposite of the 1b spectra. That is, the chemical shielding perpendicular to the symmetry axis is upfield, which is the case for carbon species with bonding perpendicular to the symmetry axis. The carbon–boron bonds to the 2c site lie 10° out of the plane perpendicular to the C_3 axis,[7] which results in significant chemical shielding in the plane.

The ^{13}C NMR spectrum of boron carbide measured during magic-angle spinning is consistent with the resolved spectra. The only feature in Figure 3 not attributed to the background signal of the rotor is the broad peak centered at ~−2 ppm. Because of the unorthodox bonding arrangement of carbon in $B_{12}C_3$ it is not possible to predict the isotropic shift at the two carbon sites. However, the peak at ~−2 ppm is comparable to the isotropic shift of the resolved spectrum in Figure 4a and thus is interpreted as the narrowed spectrum of the 2c carbons. The $^{13}C-^{11}B$ dipolar interaction for this site is 3.90 kHz, and therefore spinning at 3.90 kHz does not narrow the peak completely. This also explains why the peak at ~−2 ppm is not observed at slower (less than 3 kHz) rates of rotation. The isotropic shift of the 1b carbon atoms is predicted to be −85 ± 10 ppm and unfortunately is obscured by the background peak of the delrin. In principle, since the isotropic shifts are well-separated, it is possible to determine the distribution of carbon in samples of boron carbide by measuring the ^{13}C magic-angle spinning spectrum. It is necessary, of course, to use a rotor of a different material, such as Kel-F (poly(trifluorochloroethylene)) or ceramics, so that the spectral region near−85 ppm is not occluded.

D. Detection of Free Graphite. The presence of graphitic impurities in boron carbide can lead to inaccurate determination of the stoichiometry and crystal structure.[10] In principle, since the T_2 of graphite is an order of magnitude longer than any of the carbon sites in the boron carbide lattice, the spectrum of graphite could be isolated by the spin–echo experiment with delays set longer than 10 ms. However, at levels of ~1% graphite, the extremely weak signal, complicated by a relatively long T_1 for graphite,[24] would prohibit the detection of graphite by NMR spectroscopy with present instrumentation.

Summary

^{13}C NMR spectra of boron carbide obtained from a FID and from spin–echoes are reported. The decay of the intensities of the spectra as a function of the delay length in the spin–echo experiment is attributed to $^{13}C-^{11}B$ heteronuclear couplings. The rate of decay is determined by the strength of the homonuclear coupling within the ^{11}B spin system and the strength of the $^{13}C-^{11}B$ heteronuclear interaction at each lattice position. The experimental spin–echo decay is consistent with the crystal structure reported originally for $B_{12}C_3$;[1,2] i.e., carbon atoms occupy the 2c and 1b sites in the intericosahedral voids. Replacement of the carbon in the 1b sites with boron from a $6h_2$ site to yield $(B_{11}C)(CBC)$ would increase the $^{13}C-^{11}B$ heteronuclear coupling for both carbon species and consequently leads to a predicted spin–echo decay that is more rapid than observed. The spin–echo decay data suggest that in these samples of boron carbide, less than 10% of the 1b positions are occupied by boron.

(21) Haeberlen, U. "High Resolution NMR in Solids: Selective Averaging; Advances in Magnetic Resonance, Supp. 1"; Academic Press: New York, 1976.
(22) Zilm, K. W.; Grant, D. M. *J. Am. Chem. Soc.* **1981**, *103*, 2913.
(23) Duncan, T. M., manuscript in preparation.
(24) Carver, G. P. *Phys. Rev. B* **1970**, *2*, 2284.

The ^{13}C spectra assigned to the 2c and 1b positions overlap, but can be separated by a formalism based on differences in ^{13}C–^{11}B heteronuclear couplings. The relative areas of the resolved spectra indicate that 33 ± 5% of the carbon atoms have ^{13}C–^{11}B couplings that can be interpreted only as 1b lattice sites. The spectrum of the 1b carbon indicates axially symmetric shielding, in agreement with the threefold rotational symmetry at the site. Also, the magnitude and orientation of the chemical shielding anisotropy are comparable to that of other unsaturated carbon species with axially symmetric shielding, such as acetylene and inorganic acetylides. The ^{13}C NMR spectrum interpreted as carbon in 2c lattice positions is broadened by much stronger ^{13}C–^{11}B dipolar couplings and has about one-third the chemical shielding anisotropy as the 1b carbons. Although it is not possible to extract the precise chemical shielding components, the spectrum is consistent with the threefold symmetry of the 2c site.

The isotropic shifts of the spectra resolved and identified on the basis of the spin–echo data are ~−85 and ~−2 ppm, for the 1b and 2c carbon species, respectively. Thus, although the conventional ^{13}C NMR spectra are completely overlapped, the spectra acquired while the sample was spinning at the "magic angle" will yield two resolved peaks at the isotropic shifts. The relative areas of the peaks at −85 and −2 ppm, adjusted to compensate for the differences in chemical anisotropy at each site,[25] would indicate the distribution of carbon among the 1b and 2c sites.

Acknowledgment. The analysis of the spin–echo data benefited from discussions with Dean Douglass.

Registry No. $B_{12}C_3$, 12069-32-8.

(25) Herzfeld, J.; Berger, A. E. *J. Chem. Phys.* **1980**, *73*, 6021.

Use of Nuclear Magnetic Resonance To Investigate Bonding Interactions between Quadrupolar Nuclei. Boron–Boron Spin–Spin Coupling Constants in Linked Polyhedral Borane and Carborane Cages[1,2]

John A. Anderson,[3a] Robert J. Astheimer,[3b] Jerome D. Odom,*[3a] and Larry G. Sneddon*[3b,4]

Contributions from the Departments of Chemistry, University of South Carolina, Columbia, South Carolina 29208, and University of Pennsylvania, Philadelphia, Pennsylvania 19104.
Received September 28, 1983

Abstract: High-field boron-10 and boron-11 NMR has been used to observe boron–boron coupling in two-center, two-electron, boron–boron bonds linking coupled-cage boranes and carboranes. The values of $J_{^{11}B^{11}B}$ were found to range from 151 to ~79 Hz: 3:3′-[2,4-$C_2B_5H_6$]$_2$, 151 Hz; 1:1′-[B_5H_8]$_2$, 149 Hz; 2:2′-[1,5-$C_2B_3H_4$]$_2$, 137 Hz; 1:3′-[2,4-$C_2B_5H_6$]$_2$, 124 Hz; 1:2′-[B_5H_8]$_2$, 112 Hz; 2:1′-[1-$(CH_3)B_5H_7$][B_5H_8], 112 Hz; 3:5′-[2,4-$C_2B_5H_6$]$_2$, ≥100 Hz; and 2:2′-[B_5H_8]$_2$, ~79 Hz. To aid in the determination of the coupling, noninteractive solvents, elevated temperatures, and resolution-enhancement techniques were employed, and the utility of these techniques in analyzing the NMR line shapes of coupled quardrupolar nuclei is discussed. The boron-11 NMR spectrum of 3:5′-[2,4-$C_2B_5H_6$]$_2$ is shown to be of special interest since it was demonstrated that the unusual line shapes of the resonances arising from the linked borons are due to second-order effects resulting from strong homonuclear coupling between the two borons. It also has been shown that Kroner and Wrackmeyer's correlation between the magnitude of J_{BB} and the s character of an orbital can be used to calculate the s orbital character of the hybrid orbitals involved in the exopolyhedral boron–boron linkages. Values were found to range from 40.7% s (~$sp^{1.5}$) for $B_{3,3'}$ in 3:3′-[2,4-$C_2B_5H_6$]$_2$ to 31.8% s (~$sp^{2.2}$) for $B_{2,2'}$ in 2:2′-[B_5H_8]$_2$. Intracage boron–boron spin–spin coupling in both 2,4-$C_2B_5H_7$ and in the coupled cage boranes and carboranes was also observed and is discussed.

The tremendous impact that nuclear magnetic resonance spectroscopy has had in all areas of chemistry in well recognized. With the advent of Fourier transform methods in NMR spectroscopy and the widespread use of "broad-band" FT spectrometers, an increasing number of nuclei are being studied. An inspection of the nuclear properties of the elements reveals that 87 of 116 magnetically active isotopes have a nuclear spin value, I, greater than $^1/_2$ (i.e., are quadrupole nuclei).[5,6] The principal difficulty in NMR studies of quadrupolar nuclei is that, owing to relaxation effects, line widths can be very large, preventing the extraction of useful information that is commonly obtained in studies of spin $^1/_2$ nuclei. Perhaps because of the lack of experimental data and the complexities of the systems, theoretical studies of the NMR line shapes of quadrupolar nuclei spin–spin coupled to other quadrupolar nuclei have been lacking. However, there is an increasing recognition among chemists that modern sample and data manipulation techniques provide an effective means to study many of these chemically interesting quadrupolar nuclei.

Boron possesses two magnetically active nuclei, both of which are quadrupolar (^{10}B, I = 3, 20%; ^{11}B, I = $^3/_2$, 80%). The utility of ^{11}B NMR spectroscopy in studies of boron hydrides, carboranes, and other boron-containing compounds is well documented[7,8]

(1) Part 7 of "High Resolution Boron-11 Nuclear Magnetic Resonance Spectroscopy". For Part 6 see: Stampf, E. J.; Garber, A. R.; Odom, J. D.; Ellis, P. D. *J. Am. Chem. Soc.* **1976**, *98*, 6550–6554.
(2) Taken in part from the thesis of J. A. Anderson, submitted to the Department of Chemistry in partial fulfillment of the requirements for the Ph.D. degree.
(3) (a) University of South Carolina. (b) University of Pennsylvania.
(4) Alfred P. Sloan Foundation Fellow.
(5) Harris, R. K.; Mann, B. E., Eds. "NMR and the Periodic Table"; Academic Press: New York, 1978.
(6) Brevard, C.; Granger, P. "Handbook of High Resolution Multinuclear NMR"; John Wiley and Sons: New York, 1981.
(7) Eaton, G. R.; Lipscomb, W. N. "NMR Studies of Boron Hydrides and Related Compounds"; W. A. Benjamin: New York, 1969.
(8) Noth, H.; Wrackmeyer, B. "Nuclear Magnetic Resonance Spectroscopy of Boron Compounds"; Spinger-Verlag: Berlin, 1978.

0002-7863/84/1506-2275$01.50/0